Molecular Dynamics Simulation of Carbon and Boron Nitride nanotubes: Tensile and Compressive Behavior

Molecular Dynamics Simulation of Carbon and Boron Nitride nanotubes: Tensile and Compressive Behavior

Deepa Bedi*[1], Aditya Sharma[2], Sumit Sharma[3], S.K. Tiwari[4]

[1]Research Scholar, Department of Mechanical Engineering. Dr. B R Ambedkar National Institute of Technology Jalandhar, Punjab, India
[2]Research Scholar, Department of Mechanical Engineering. Dr. B R Ambedkar National Institute of Technology Jalandhar, Punjab, India
[3]Research Scholar, Department of Mechanical Engineering. Dr. B R Ambedkar National Institute of Technology Jalandhar, Punjab, India
[4]Research Scholar, Department of Mechanical Engineering. Dr. B R Ambedkar National Institute of Technology Jalandhar, Punjab, India
[1]E-mail address: deepab.me.19@nitj.ac.in

Abstract. In this paper, the mechanical properties of Carbon nanotubes (CNTs) and Boron Nitride nanotubes (BNNTs) are studied systematically by using molecular dynamics simulations. CNTs are considered semi-metallic, whereas the BNNTs, of the large band gap, are considered to be insulators, regarding the difference in the electrical properties of CNTs and BNNTs; comparing the mechanical properties of both nanotubes offers great scientific significance for their prospective applications. The simulations were carried out with the help of a Large-scale atomic/molecular massively parallel simulator (LAMMPS) and were based on the Airebo and Tersoffs force fields for C-C interaction in CNTs and B-N interaction in BNNTs, respectively. Failure behavior of armchair and zigzag CNTs and BNNTs under tensile and compressive loading has been predicted and observed that for both the nanotubes the armchair nanotubes showed higher tensile and compressive strength as compared to zigzag nanotubes. The maximum tensile and compressive strength for CNTs is 205 GPa and 35.62 GPa respectively and for BNNTs are 159 GPa and 24.81 GPa respectively. CNTs are identified as axially stronger and stiffer than BNNTs for the same diameter under identical loading conditions.

Keywords: Molecular Dynamics, Modeling, LAMMPS, Tensile strength, Compressive strength

1. Introduction

Carbon nanotubes have a hexagonal lattice structure like that of graphene, and were discovered by Iijima in 1991 through arc – the discharge evaporation method in which needle-like structures grow at the negative end of an electrode whose inspection through electron microscopy revealed that each structure consisted of coaxial graphitic sheets varying 2 – 50 in number Iijima [1]. CNTs may be thought of as graphene sheets rolled up into a hollow cylinder, which may be of a Single-Walled CNT, and if there is more than one sheet then it is called Multi-Walled Carbon NTs. The aspect ratio or L/D ratio of NTs can be as high as $10^4 – 10^5$ therefore nanotubes are usually considered to be 1-D structures [2].

Boron Nitride is a diatomic compound consisting of Group 3 and Group 5 elements of the periodic table which due to properties like similarity in polymorphism and specific structure is closest to the C system as compared to other compounds of elements from the same Groups. Boron nitride nanotubes were soon discovered after the discovery of CNTs, efforts were made to obtain another compound having a similar layered structure as CNT and it was in 1995 when BNTs were synthesized by the same arc-discharge method which was sp^2 hybridized and hexagonally bonded, replacing the C – C with B – N bonds bonded alternatively [3]. BN compounds are analogs of Carbon compounds. Due to the electronegativity difference between the two atoms namely B and N, these compounds possess some dipole moment which affects the molecular and solid state chemistry of the compounds along with the optical properties [4, 5].

CNTs and BNNTs have different appearances, CNTs are purely black whereas BNNTs are white, and maybe yellowish sometimes. CNTs can be metallic or sometimes may be employed as narrow band-gap semiconductors [6]. BNNTs offer better insulation owing to the large band gap ranging from 5.0 to 6.0 eV which is independent of tube chirality [5, 7]. Both these compounds exhibit excellent mechanical properties, researchers over the years have found the Young's Modulus of both these compounds to touch

the level of TPa. The Young's Modulus of BNNTs is somewhat lower than that of CNTs, ranging between 0.7 – 0.9 TPa [8].

Since both the materials have different properties from an electronics perspective, there are discrepancies in the usage of both the compounds, for instance, BNNTs are better fillers for insulating materials which results in a better reduction of coefficient of thermal expansion[9] while CNTs are useful for enhancement of electrical conductivity of polymers [10]. Moreover, BNNTs are thermally more stable than CNTs, and BNNTs possess more oxidation stability than CNTs too [11, 12]. However, both can be used in place of one another due to similarities in properties like similar hexagonal structure, for example, improvement of thermal conductivity or usage as reinforcement material for composite matrix. BNNTs are still unexplored than CNTs owing to a lack of experiments and research in this particular direction. Growing large quantities of pure single-walled BNTs still poses a challenge, and fabrication of such BNTs through methods that work for CNTs proves to be largely inefficient [13, 14].

Experiments over the years have confirmed that nanotubes are exceptionally stiff along the longitudinal or axial direction and are considered good at bending therefore the nanotubes are capable of sustaining large loads without failure. In a study by Li, Tang et al. 2017 [15] simulations were made on (10, 0), (10, 10) and (20, 0) CNTs and BNNTs, and the lengths of C – C and B – N bonds were taken to be 0.142 nm and 0.145 nm respectively. The values of Young's Moduli were found to be 1.1 TPa for CNTs and 0.72 TPa for BNNTs which is nearly 34.5 % smaller than that of CNTs proving that the CNTs are stiffer than BNNTs in longitudinal the direction. In another study carried out by Vaccarini [12] on SWNTs of different chirality, the study exhibited that Young's Modulus of the nanotube which reflects its stiffness in axial direction tends to depend on the diameter (experimental range of 1.3 – 1.4 nm) and chirality of the nanotube. The results predicted that CNTs have the highest Young's Modulus of all the considered nanotubes, i.e. 1.26 TPa. Other studies[8, 16] also show that the range of Young's Modulus for CNTs ranges from 1.22 – 1.25 TPa irrespective of the chirality, and for that of BNNTs the range falls to 0.837 – 0.912 TPa.

A study by Peng et al. [17] shows that a sudden or abrupt drop in strain energy or force detects the buckling stage. This drop occurs as a result of significant structural and geometrical variations of Carbon Nanotubes associated with the energy release of CNTs. In another study by Goel et al. [18] simulations were made on LAMMPS to carry out axial compression of pristine CNT where it was observed that before buckling compressive force linearly varies with axial strain and strain energy.

The current study focuses on the study of axial strain mechanical behavior of CNTs and BNNTs of different chirality through Molecular Dynamics (MD) simulation by using LAMMPS. Although the manufacturing of pristine or defect-free CNTs and BNNTs is quite a difficult task still there is a need to determine values for defect-free nanotubes so that deviation can be known for defected nanotubes. The simulations are carried out on chirality (n, n) or Armchair type and (n, 0) chiral nanotube namely Zig-Zag. Study is focused on three types, Armchair of (5, 5), (10, 10), and (15, 15) and Zig-Zag of (5, 0), (10, 0), (15, 0). BNNTs and CNTs are formed using open-source VMD software as Hexahexa-angular carbon rings to obtain the dependence of mechanical properties on its chiral directions.

2. MD computational modeling of CNTs and BNNTs:

The armchair (5,5); (10,10); and (15,15) and zigzag (5,0); (10;0); and (15,0) CNTs and BNNTs with a constant length of 10nm were used in the current work to compare the mechanical behavior of both the nanotubes. To conduct all the MD simulations, a Large-scale atomic/molecular massively parallel simulator (LAMMPS) [19], which is open-source software, was employed. It is important to select an adequate interatomic potential capable of modeling complex systems effectively under loading conditions of dynamic nature. To characterize the interactions between C–C atoms and B–N atoms, generalized Airebo [20] potentials and Tersoff [21] potentials were used, which produce remarkably precise findings for the mechanical properties of C and BN nanostructures. SWCNTs and BNNTs were created as Hexa-angular carbon and boron rings, respectively, using open-source VMD software to accomplish mechanical property dependence on chiral orientations. The VMD software generated a data file comprising the Cartesian coordinates of carbon atoms of SWCNT and Boron nitrogen atoms of BNNT. Both Armchair and Zigzag CNTs and BNNTs were modeled to obtain the Young's Modulus, ultimate strength, critical failure, and buckling strain under axial tension and compression loading.

The simulation uses a 0.1 fs integration time step and periodic boundary conditions (PBC) in all three dimensions with vacuum surfaces large enough in the radial directions of the nanotube to exclude the impacts of nearby atoms. PBC applied in the loading direction may reduce finite length effects and offer correct uniaxial stress conditions. The conjugate gradient minimization method was used to minimize the

energy and obtain the optimized structure of CNT and BNNT. The system is then configured to 300 K for 200 ps within the NVT ensemble over a time step of 1femtosecond and the velocity Verlet algorithm was used to integrate Newton's equations of motions. By using the NPT ensemble, the constant pressure of zero was maintained during the relaxation period. The Nosé–Hoover thermostat was employed to regulate the pressure and temperature, which prevent the CNTs and BNNTs from thermally expanding [22].

Figure 1 (a) and (b) show the pristine armchair and zigzag CNT and figure 2 (a) and (b) represent the pristine armchair and zigzag BNNT under the axial tensile and compressive loading respectively in the z-direction. To suppress rigid body rotation, the left side atoms of both types of nanotubes were clamped, while the atoms on the right side were subjected to uniaxial tensile and compressive loading in the armchair and zigzag direction subsequently to predict the tensile and compressive behavior of CNTs and BNNTs. For drawing a comparison between the failure mechanics of single-wall CNTs and BNNTs the stress-strain distribution during the deformation were observed in the axial direction under the tensile and compressive loading.

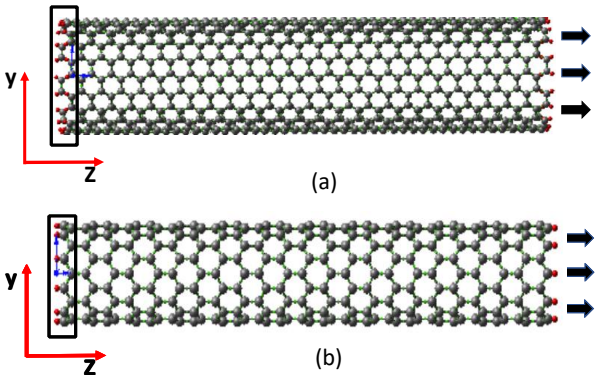

Figure 1: schematic view of (a) Armchair CNT (b) Zigzag CNT, under tensile loading.

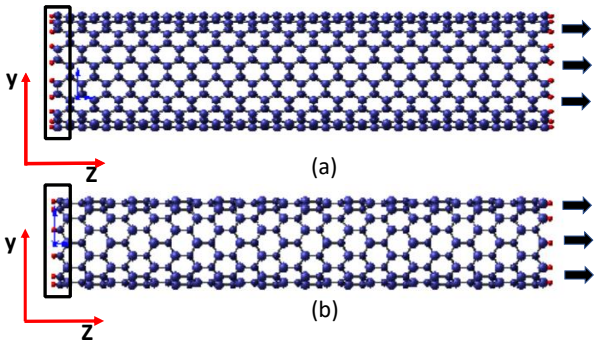

Figure 2: schematic view of (a) Armchair BNNT (b) Zigzag BNNT, under tensile loading.

3. Result and Discussion:

In this study carried out in this paper, armchair and zigzag CNTs and BNNTs with varying diameters were considered to predict and compare the mechanical properties of nanotubes. Figure 3(a) and (b) and figure 4 (a) and (b) shows the stress-strain behaviour of (5,5); (5,0); (10,10); (10,0) and (15,15); (15,0) CNTs and BNNTs respectively under tensile loading and compressive loading. It has been observed from the graphs that stress increases linearly with increasing strains in the first stage. When the strain value is increased to the critical failure and buckling strain, the corresponding stress drops rapidly, then progressively falls as the strain value is increased. Finally, with more tension and compression, stress remains nearly unaltered and approaches a constant value. The stress vs strain behavior of armchair and zigzag CNTs and BNNTs predicted by the current study signifies the same trend has been obtained by li et al. [23] under compression

and choyal et al [24] [25] under tension. The obtained elastic properties of CNTs and BNNTs such as Ultimate strength, failure strain and buckling strain are listed in table 1. Irrespective of chiralities and diameters, the predicted Young's Modulus for CNTs is around 1.1-1.2 TPa and 0.72-0.80 TPa for BNNTs. BNNTs have Young's Modulus that is roughly 30.0 percent lower than the CNTs. The maximum stress for a CNT is higher than for a BNNT of the same diameter, indicating that CNTs are stronger and axially stiffer than BNNTs. It has been observed from the results that maximum stress is related to diameters of both CNTs and BNNTs, demonstrating the axial deformation behaviors of Carbon (C) and Boron Nitride (BN) nanotubes are size dependent.

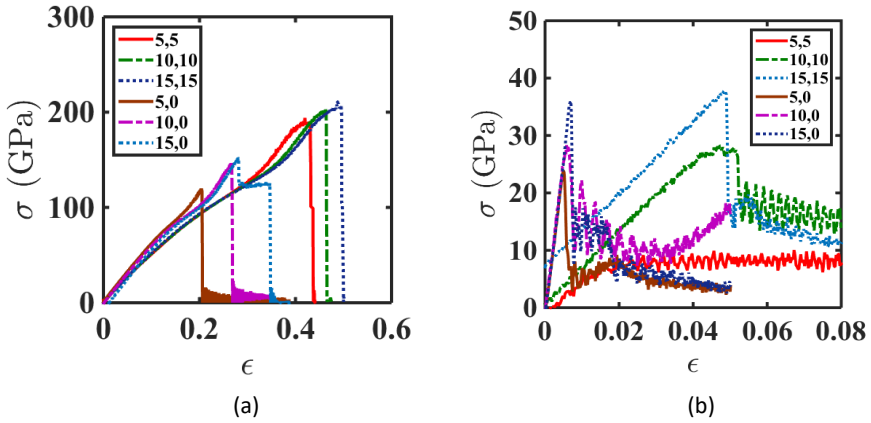

Figure 3: Uniaxial stress-strain relation of armchair (AC) and zigzag (ZZ) CNTs (a) under Tensile loading (b) under Compressive loading.

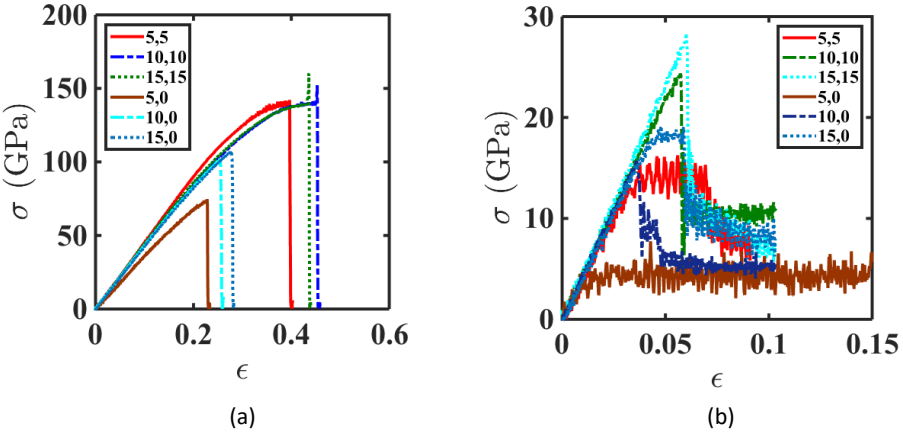

Figure 4: Uniaxial stress-strain relation of armchair (AC) and zigzag (ZZ) BNNTs (a) under Tensile loading (b) under Compressive loading.

Table 1 Ultimate Tensile and Compressive strength and strain of BNNT and CNT.

Chirality	**BNNT**				**CNT**			
	Tensile		**Compressive**		**Tensile**		**Compressive**	
	Stress (GPa)	**Strain**	**Stress (GPa)**	**Strain**	**Stress (GPa)**	**Strain**	**Stress (GPa)**	**Strain**
(5, 5)	141.3838	0.3963	16.2450	0.0559	188.9651	0.4304	10.7	0.064
(10, 10)	150.8330	0.4525	24.1813	0.0547	204.2961	0.4628	29.43	0.051
(15, 15)	159.8168	0.4355	15.4107	0.0363	210.5456	0.4953	38.7240	0.052

(5, 0)	74.309	0.2280	7.7492	0.0492	117.2394	0.2051	22.13	0.019
(10, 0)	101.36507	0.2456	19.0875	0.0587	144.7644	0.2666	27.8929	0.018
(15,0)	106.5667	0.2778	27.4141	0.0600	149	0.27	37.0	0.019

It has been observed from the results that until the critical buckling strain (in compressive case) and fracture point (in tensile case) come into the picture the stress vs strain curve is approximately linear and followed a trend similar to Hooke's law. The curves are overlapping for short strain values for example it can be seen that up to a strain value of 0.155 the curves for different chirality of CNTs are nearly indistinguishable. At a certain point, the curve falls sharply at nearly constant strain for both types of loadings that is, strain remains unchanged for decreasing stress values, which can be interpreted as the component's failure point. In the case of tensile loadings stress after fracture falls to zero value nearly which means that the nanotube may rupture at this value. In compressive loading, after increasing to critical buckling strain, the curve falls sharply and then the slow reduction is observed with increasing strain values and stress values don't change for further increase in compressive load and hence attain a constant value.

Both CNT and BNNT have similar behavior under the same loading circumstances because they possess almost similar structures, C-C bonds are hexagonally bonded in a single plane in CNTs and a similar pattern is followed by BNNTs where B and N atoms replace C atoms alternatively. Figure 5 and figure 6 represents the axial deformation behavior of 10,10 armchair CNTs under tensile and compressive loading at different value of strain respectively. Initially, with the application of tensile load, nanotubes tend to show necking behavior after the ultimate stress point and when the load is further increased fracture takes place. A similar case is with compressive loading but in place of necking, nanotubes tend to wrinkle from the region around the mid length and failure happens through buckling.

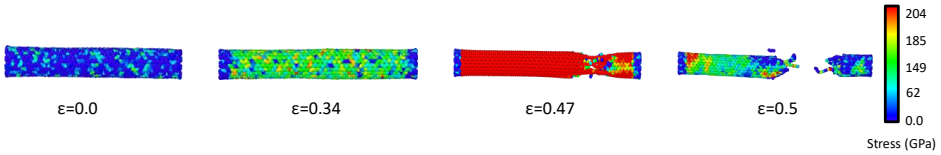

Figure 5 Progressive failure analysis of pristine armchair (10,10) CNT under uniaxial tensile loading at different strains.

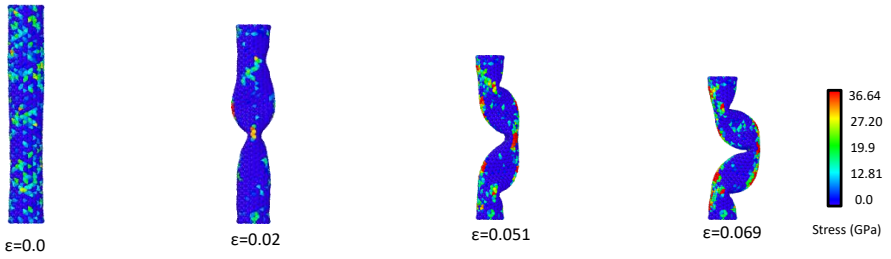

Figure 6 Progressive buckling behavior of pristine armchair (10,10) CNT under uniaxial compressive loading at different strains.

It can be concluded that BNNTs show buckling behavior faster than CNNTs because of low critical buckling strain values. Also, it is observable that for the same orientation, stress and strain values (tensile or compressive) are greater in the case of CNTs than that of BNNTs proving that CNTs are stronger and stiffer than BNNTs for the same chirality and thus CNTs can sustain longer than BNNTs for same loading conditions.

Zhi, Bando et al. [5] calculated the young's modulus values for (10, 0); (10, 10); and (15, 15) CNTs as 0.416, 0.423 and 0.425 TPa. We calculated the values to be 0.544, 0.433, and 0.404 TPa which are by the reference mentioned before. Similarly, for BNNTs the range comes out to be 0.244 – 0.295 which is again by the values in reference. Therefore, the values so calculated from simulation through molecular dynamics are verified with values from previous works.

4. Conclusion

In the current study, MD simulations employing the LAMMPS software are used to investigate and compare the mechanical properties of the armchair and zigzag CNTs and BNNTs. Stress-strain curves and deformation behaviors of CNTs and BNNTs under axial tensile and compressive loading are evaluated to predict the mechanical behavior, with different diameters and chirality and found to be that the maximum stress and critical buckling strain of both the nanotubes are related to diameter and chirality. CNTs have Young's modulus of roughly 1.3 TPa, while BNNTs have Young's modulus of 0.72 TPa, which concluded that CNTs are axially stronger and stiffer than BNNTs.

Following conclusions have been drawn from the simulation

a. With increasing the diameter of both the nanotube the value of ultimate strength increases.
b. The armchair nanotubes had a higher value of strength and strain under tensile loading as compared to zigzag nanotubes.
c. CNTs are stronger and stiffer than BNNTs under identical conditions.

These findings provide important guidance for CNTs, BNNTs, and their composites' prospective uses in micro/nano-electro-mechanical systems.

Data availability

Due to legal and ethical constraints, the raw/processed data needed to replicate these findings and results cannot be disclosed at this point in time. However, this data will be made available, if requested.

Acknowledgment

The researchers are grateful to Dr. BR Ambedkar National Institute of Technology Jalandhar, Department of Mechanical Engineering for providing computational resources for this study.

References

[1] Iijima S 1991 *Nature* **354** 56-58
[2] Bedi H S, Tiwari M and Agnihotri P K 2018 *Carbon* **132** 181-190
[3] Chopra N G, Luyken R J, Cherrey K, Crespi V H, Cohen M L, Louie S G and Zettl A 1995 *science* **269** 966-967
[4] Akdim B, Pachter R, Duan X and Adams W W 2003 *Physical Review B* **67** 245404
[5] Zhi C, Bando Y, Tang C and Golberg D 2010 *Materials Science and Engineering: R: Reports* **70** 92-111
[6] Mintmire J W, Dunlap B I and White C T 1992 *Physical Review Letters* **68** 631
[7] Terrones M, Romo-Herrera J, Cruz-Silva E, Lopez-Urias F, Munoz-Sandoval E, Velázquez-Salazar J, Terrones H, Bando Y and Golberg D 2007 *Materials today* **10** 30-38
[8] Hernandez E, Goze C, Bernier P and Rubio A 1998 *Physical Review Letters* **80** 4502
[9] Zhi C, Bando Y, Terao T, Tang C, Kuwahara H and Golberg D 2009 *Advanced Functional Materials* **19** 1857-1862
[10] Park H J, Oh K A, Park M and Lee H 2009 *The Journal of Physical Chemistry C* **113** 13070-13076
[11] Balandin A A 2011 *Nature materials* **10** 569-581
[12] Vaccarini L, Goze C, Henrard L, Hernandez E, Bernier P and Rubio A 2000 *Carbon* **38** 1681-1690
[13] Golberg D, Bando Y, Tang C and Zhi C 2007 *Advanced Materials* **19** 2413-2432
[14] Golberg D, Bando Y, Huang Y, Terao T, Mitome M, Tang C and Zhi C 2010 *ACS Nano* **4** 2979-2993
[15] Li T, Tang Z, Huang Z and Yu J 2017 *Physica E: Low-dimensional Systems and Nanostructures* **85** 137-142
[16] Hernandez E, Goze C, Bernier P and Rubio A 1999 *Applied Physics A* **68** 287-292
[17] Peng X and Meguid S 2017 *European Polymer Journal* **93** 246-258
[18] Goel M, Harsha S P, Mishra M P and Mishra R K 2020 *Journal of Failure Analysis and Prevention* **20** 868-881
[19] Plimpton S 1995 *Journal of computational physics* **117** 1-19
[20] Stuart S J, Tutein A B and Harrison J A 2000 *The Journal of chemical physics* **112** 6472-6486
[21] Lindsay L and Broido D 2010 *Physical Review B* **81** 205441
[22] Dewapriya M, Rajapakse R and Dias W 2020 *Carbon* **163** 425-440

[23] Li T, Tang Z, Huang Z and Yu J 2017 *Physica E: Low-Dimensional Systems Nanostructures* **85** 137-142
[24] Choyal V and Kundalwal S 2020 *Acta Mechanica* **231** 4003-4018
[25] Kundalwal S and Choyal V 2018 *Acta Mechanica* **229**